A Catalytic Triad Is Responsible for Acid−Base Chemistry in the *Ascaris suum* NAD−Malic Enzyme†

William E. Karsten,‡ Dali Liu,‡ G. S. Jagannatha Rao,§ Ben G. Harris,§ and Paul F. Cook*,‡

Department of Chemistry and Biochemistry, University of Oklahoma, 620 Parrington Oval, Norman, Oklahoma 73019, and Department of Molecular Biology and Immunology, University of North Texas Health Sciences Center, 3500 Camp Bowie Boulevard, Fort Worth, Texas 76107

Received October 8, 2004; Revised Manuscript Received November 29, 2004

ABSTRACT: The pH dependence of kinetic parameters of several active site mutants of the *Ascaris suum* NAD−malic enzyme was investigated to determine the role of amino acid residues likely involved in catalysis on the basis of three-dimensional structures of malic enzyme. Lysine 199 is positioned to act as the general base that accepts a proton from the 2-hydroxyl of malate during the hydride transfer step. The pH dependence of V/K_{malate} for the K199R mutant enzyme reveals a p*K* of 5.3 for an enzymatic group required to be unprotonated for activity and a second p*K* of 6.3 that leads to a 10-fold loss in activity above the p*K* of 6.3 to a new constant value up to pH 10. The *V* profile for K199R is pH independent from pH 5.5 to pH 10 and decreases below a p*K* of 4.9. Tyrosine 126 is positioned to act as the general acid that donates a proton to the enolpyruvate intermediate to form pyruvate. The pH dependence of V/K_{malate} for the Y126F mutant is qualitatively similar to K199R, with a requirement for a group to be unprotonated for activity with a p*K* of 5.6 and a partial activity loss of about 3-fold above a p*K* of 6.7 to a new constant value. The Y126F mutant enzyme is about 60000-fold less active than the wild-type enzyme. In contrast to K199R, the *V* rate profile for Y126F also shows a partial activity loss above pH 6.6. The wild-type pH profiles were reinvestigated in light of the discovery of the partial activity change for the mutant enzymes. The wild-type V/K_{malate} pH−rate profile exhibits the requirement for a group to be unprotonated for catalysis with a p*K* of 5.6 and also shows the partial activity loss above a p*K* of 6.4. The wild-type *V* pH−rate profile decreases below a p*K* of 5.2 and is pH independent from pH 5.5 to pH 10. Aspartate 294 is within hydrogen-bonding distance to K199 in the open and closed forms of malic enzyme. D294A is about 13000-fold less active than the wild-type enzyme, and the pH−rate profile for V/K_{malate} indicates the mutant is only active above pH 9. The data suggest that the p*K* present at about pH 5.6 in all of the pH profiles represents D294, and during catalysis D294 accepts a proton from K199 to allow K199 to act as a general base in the reaction. The p*K* for the general acid in the reaction is not observed, consistent with rapid tautomerization of enolpyruvate. No other ionizable group in the active site is likely responsible for the partial activity change observed in the pH profiles, and thus the group responsible is probably remote from the active site and the effect on activity is transmitted through the protein by a conformational change.

Malic enzyme is a member of a class of pyridine nucleotide-linked enzymes that catalyze the oxidative decarboxylation of β-hydroxy acids (*1*). The enzyme catalyzes the oxidative decarboxylation of L-malate to give pyruvate and CO_2 using $NAD(P)^+$ as the oxidant. A general acid/base mechanism has been proposed for the *Ascaris suum* NAD−malic enzyme on the basis of the pH dependence of kinetic parameters and isotope effects (*2*−*5*). There are three major chemical steps in the overall reaction. Malate is first oxidized to oxalacetate assisted by an enzyme group acting as a general base. The same residue participates in all three steps acting as a proton shuttle between the C2 hydroxyl and itself. The oxalacetate intermediate is then decarboxylated by a Lewis acid assist from the divalent metal ion (Mg^{2+}), and this is followed by tautomerization of the resulting enolpyruvate, which is protonated by the second enzyme group acting as a general acid. The mechanism is shown in Scheme 1.

In previous studies, we have proposed that D295 acts as the general base (*6*) and K199 acts as the general acid on the basis of site-directed mutagenesis prior to the availability of a three-dimensional structure of the malic enzyme (*7*). In addition, we have proposed that the general acid group also contributes to malate binding by interacting with the β-carboxyl group of L-malate and plays an important role in the isomerization step preceding catalysis. Another residue, Y126, in close proximity to K199, was assigned a structural

† This work was supported by grants from the NSF (MCB 0091207) and the Oklahoma Center for the Advancement of Science and Technology (HR99-081) to P.F.C., grants from the NIH (AI24155, AI41552) and the Robert A. Welch Foundation (BK1309) to B.G.H., and funds for P.F.C. from an endowment to the University of Oklahoma to fund the Grayce B. Kerr Centennial Professorship in Biochemistry.

* Corresponding author. Tel: 405-325-4581. Fax: 405-325-7182. E-mail: pcook@chemdept.chem.ou.edu.

‡ University of Oklahoma.

§ University of North Texas Health Sciences Center.

10.1021/bi047826o CCC: $30.25
Published on Web 02/09/2005

Scheme 1: Proposed Mechanism of Malic Enzyme

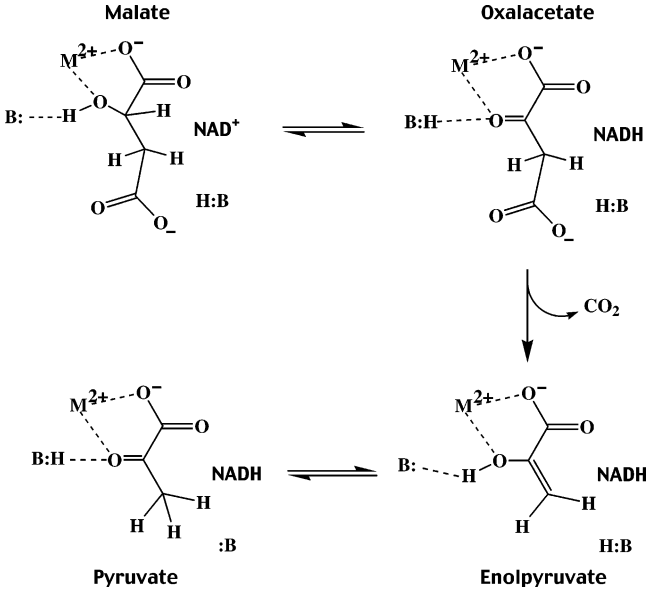

role. The structure of the mitochondrial NAD−malic enzyme from *A. suum* has been solved with NAD^+ bound to the active site (*8*). Three-dimensional structures of the human mitochondrial NAD−malic enzyme have recently been published (*9*−*14*). An "open" form has been obtained with NAD^+ bound to the active site and an allosteric inhibitory site, and a "closed" form has been solved with NAD, Mn^{2+}, and oxalate (or ketomalonate, or tartronate) bound at the active site and NAD bound at the allosteric site. Additional closed structures of the human mitochondrial NAD−malic enzyme have been solved with Mn^{2+}, malate, and NADH or Mn^{2+}, NAD, and pyruvate bound at the active site. These structures show K183 (K199 in the *Ascaris* enzyme) within hydrogen-bonding distance to the C2 hydroxyl (or carbonyl for ketone substrates or analogues) of the substrate and positioned properly to act as the general base in the oxidative decarboxylation reaction. Tyrosine 112 (Y126 in the *Ascaris* enzyme) is positioned to act as the general acid. In these closed structures K183 is also hydrogen bonded to Y112 and D278 (D294 in the *Ascaris* enzyme). D278 is also within hydrogen-bonding distance of E255 (E271 in the *Ascaris* enzyme) that is also a ligand to the bound Mn^{2+}. In the open E·NAD *Ascaris* structure K199 is still within hydrogen-bonding distance to D294 (2.5 Å) but is about 4.5 Å from Y126, suggesting no interaction between these two residues. In the open structure E271 and D294 are 4.5 Å from each other. The human enzyme exhibits similar distances.

In the present study, to probe the roles of K199, Y126, and D294, additional more complete characterizations of the K199R, Y126F, and D194A mutant enzymes have been carried out using the pH dependence of kinetic parameters and isotope effects. The results from the studies on the mutant enzymes also prompted a reexamination of the pH dependence of the recombinant wild-type enzyme. The data are interpreted in the context of the available structural information on the enzyme.

MATERIALS AND METHODS

Chemicals and Enzymes. The wild-type and K199R, Y126F, R105A, and D294A mutant enzymes were prepared, expressed, purified, and characterized as reported previously (*6*). Protein concentrations were determined according to Bradford using the Bio-Rad protein assay kit with bovine serum albumin as a standard (*15*). Buffers, including *N*,*N*′-bis(hydroxyethyl)piperazine, Mes,[1] Pipes, Hepes, Taps, and Caps, were from Research Organics. All other chemicals used were obtained from commercial sources, were of the highest quality available, and were used without further purification. L-Malate-2-*d* was synthesized according to the method of Viola et al. (*16*).

Initial Velocity Studies. All initial velocity data were collected using a Beckman DU 640 spectrophotometer or a Hewlett-Packard 8453 diode array spectrophotometer to monitor the appearance of NADH at 340 nm ($\epsilon = 6220\ M^{-1}\ cm^{-1}$). All assays were carried out at 25 ± 0.1 °C, and the temperature was maintained using a circulating water bath with the capacity to heat and cool the cell compartment. Typical assays contained 100 mM Hepes, pH 7.3, 200 mM free[2] Mg^{2+} (added as $MgSO_4$), and variable concentrations of free malate (0.25−10 mM) and free NAD (10−100 μM) or 0.5 mM free NAD and variable free Mg^{2+} (5−50 mM) and free malate (0.25−10 mM). All substrate concentrations reported in the text refer to the free, uncomplexed, reactant concentration.

pH Studies. To determine whether the kinetic mechanism changes with pH, initial velocity patterns were measured at the extremes of pH (data not shown). The kinetic mechanism of the mutant enzymes is pH independent. Buffers used to obtain the pH dependence of kinetic parameters include the following: *N*,*N*′-bis(hydroxyethyl)piperazine, 4.0−5.5; Mes, 5.5−6.5; Pipes, 6.5−7.5; Hepes, 7.0−8.0; Taps, 8−9; Ches, 9−10; Caps, 10−11. Sufficient overlap was obtained as buffers were changed to correct for spurious effects, and none were observed. In some cases mixed buffers, Homopipes/Mes, Mes/Hepes, Hepes/Taps, or Taps/Caps, were used in the assays to span pH values between the pH of the stock buffers. The total buffer concentration was maintained at 100 mM. All buffers were titrated to the appropriate pH with KOH. Above pH 9, NAD was added to the reaction mixture just prior to the addition of the enzyme to minimize the base-catalyzed degradation of NAD. The pH of the reaction mixture was measured before and after the reaction, and no significant change was noted. No significant effect of ionic strength was observed up to 3.5 M. The kinetic parameters *V* and *V*/*K* are displayed as the log parameter vs pH.

Primary Deuterium Isotope Effects. Primary deuterium isotope effects were measured in the initial velocity assays in which the deuterated substrate used was L-malate-2-*d*. Initial velocity assays for deuterium isotope effects contained 100 mM Hepes, pH 7 (or 100 Taps, pH 9), 2 mM free NAD, 50 mM free Mg^{2+} (added as $MgSO_4$), and 2−20 mM L-malate-2-*h*/*d*, and the reaction was initiated by the addition of an appropriate amount of enzyme, dependent on activity. The isotope effects were estimated by direct comparison of

[1] Abbreviations: Caps, 3-(cyclohexylamino)-1-propanesulfonic acid; Ches, 2-(*N*-cyclohexylamino)ethanesulfonic acid; Hepes, *N*-(2-hydroxyethyl)piperazine-*N*′-2-ethanesulfonic acid; Homopipes, homopiperazine-*N*,*N*′-bis(2-ethanesulfonic acid); Mes, 2-(*N*-morpholino)ethanesulfonic acid; NAD, nicotinamide adenine dinucleotide; Pipes, piperazine-*N*,*N*′-bis(2-ethanesulfonic acid); Taps, 3-[tris(hydroxymethyl)amino]propanesulfonic acid.

[2] Free indicates concentration corrected for Mg−malate, Mg−NAD, and Mg−buffer chelate complexes (17).

the initial rate, varying malate at saturating concentrations of NAD and Mg^{2+}.

^{13}C Isotope Effects and Multiple Isotope Effects. The technique employed for the determination of primary ^{13}C kinetic isotope effects is that of O'Leary (*18*) as modified by Weiss et al. (*4*). The natural abundance of ^{13}C in the C-4 position of L-malate is used. Both high-conversion (100%) and low-conversion (~15%) samples were collected. A low-conversion reaction had a total volume of 40 mL, containing 50 mM Mes, pH 6 (Ches, pH 9), 12 mM malate (or malate-2-*d*), 10 mM $MgSO_4$, and 10 mM NAD. A high-conversion sample has the same components, with the exception that the concentration of malate or malate-2-*d* was decreased to 2 mM. An appropriate amount of enzyme was used, and concentrated sulfuric acid was used to quench the reaction when the desired percent completion of reaction was reached. After determining the $^{12}C/^{13}C$ isotope ratios in the CO_2 produced in the malic enzyme reaction, the ^{13}C kinetic isotope effect was calculated according to Weiss et al. (*4*).

Data Processing. Initial velocity data were fitted using the appropriate rate equation and BASIC versions of the Fortran programs developed by Cleland (*19*). Saturation curves for reactants were fitted using eq 1. Data conforming to a sequential initial velocity pattern were fitted using eq 2, and data conforming to an equilibrium ordered mechanism were fitted using eq 3.

$$v = \frac{VA}{K_a + A} \tag{1}$$

$$v = \frac{VAB}{K_{ia}K_b + K_aB + K_bA + AB} \tag{2}$$

$$v = \frac{VAB}{K_{ia}K_b + K_bA + AB} \tag{3}$$

In eqs 1, 2, and 3, v and V represent initial and maximum velocities, A and B represent reactant concentrations, K_a and K_b are Michaelis constants for A and B, and K_{ia} is the dissociation constant for A. Data for pH−rate profiles were fitted using the equations:

$$\log Y = \log\left[C/\left(1 + \frac{H}{K_1} + \frac{K_2}{H}\right)\right] \tag{4}$$

$$\log Y = \log\left[C/\left(1 + \frac{H}{K_1}\right)\right] \tag{5}$$

$$\log Y = \log\left[\frac{Y_L + Y_H\left(\frac{K}{H}\right)}{1 + \frac{K}{H}}\right] \tag{6}$$

In eqs 4, 5, and 6 Y is V or V/K, C represents the pH-independent value of Y, Y_L and Y_H are the pH-independent values of Y at low and high pH, respectively, and H is proton concentration, while K_1 and K_2 are the acid dissociation constants for enzyme or substrate functional groups that must be unprotonated or protonated, respectively, for activity.

Data for primary deuterium kinetic isotope effects were fitted using the equation

$$v = \frac{VA}{K_a(1 + F_iE_{V/K}) + A(1 + F_iE_V)} \tag{7}$$

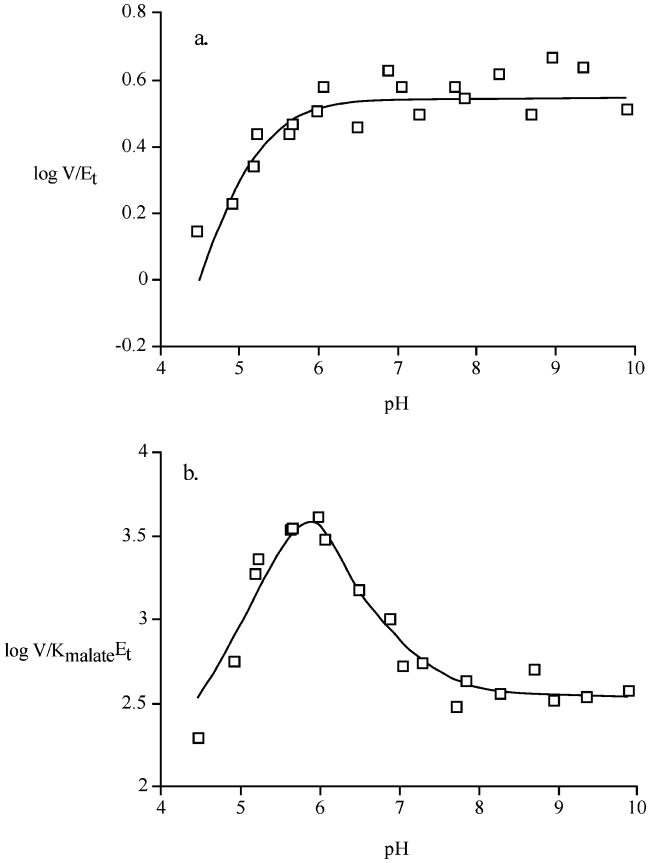

FIGURE 1: pH dependence of kinetic parameters for the K199R mutant enzyme. Initial rates were measured at saturating concentrations of NAD (2 mM) and Mg^{2+} (100 mM). The malate concentration was varied from 0.5 to 50 mM. The concentration of K199R was 53 nM. Points are the experimental values, while curves are theoretical based on a fit of the data for V (a) to eq 5 and for V/K_{malate} (b) to eqs 5 and 6.

where F_i represents the percent deuterium label in the substrate, and $E_{V/K}$ and E_V are the isotope effects minus 1 on V/K and V, respectively. The isotope effects are written as ^DV and $^D(V/K)$ according to Northrop (*20*) and Cook and Cleland (*21*). The relative rates of reaction for ^{12}C versus ^{13}C were calculated according to the equation (*4*):

$$^{13}\left(\frac{V}{K_{malate}}\right) = \frac{\log(1 - f)}{\log\left(1 - f\left(\frac{R_p}{R_o}\right)\right)} \tag{8}$$

where f is fraction of reaction, R_p is the isotopic ratio from the product of the partial reaction, and R_o is the isotopic ratio in the starting material (determined from the $^{12}C/^{13}C$ ratio at 100% reaction completion).

RESULTS

pH−Rate Profiles. The pH dependence of the V and V/K_{malate} obtained for the K199R mutant enzyme is shown in Figure 1. The V pH−rate profile is pH independent over the pH range 6.5−10 with a pH-independent value of 3.5 s^{-1}, 10% that obtained for the wild-type enzyme. The maximum rate decreases at low pH, giving a pK of 4.9 ± 0.3. On the other hand, the V/K_{malate} is pH dependent and exhibits complex behavior. The V/K_{malate} decreases at low pH with a limiting slope of 2 and gives two identical pK

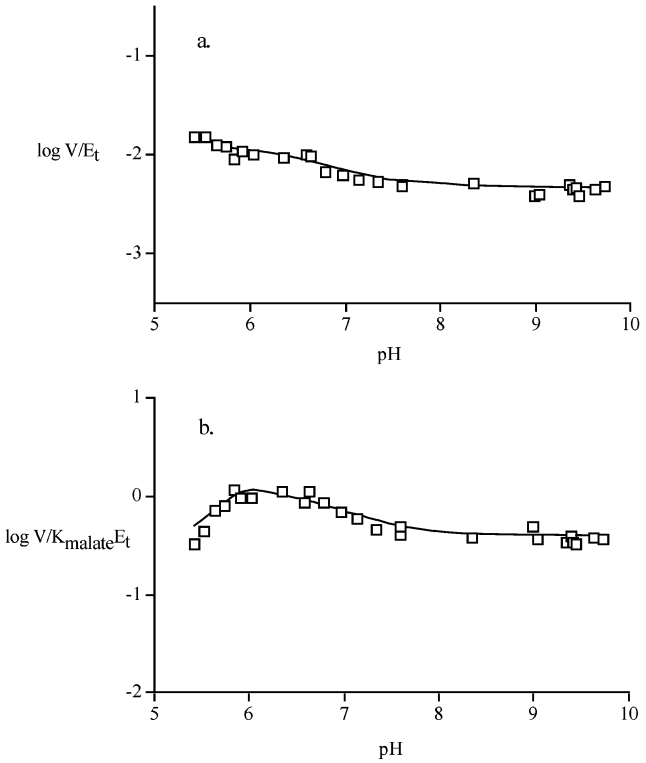

FIGURE 2: pH dependence of kinetic parameters for the Y126F mutant enzyme. Initial rates were measured at saturating concentrations of NAD (0.5 mM) and Mg^{2+} (200 mM). The malate concentration was varied from 5 to 50 mM. The concentration of Y126F was 1.9 μM. Points are the experimental values, and the curves are based on a fit of the data for V (a) to eq 6 and for V/K_{malate} (b) to eqs 5 and 6.

values, one of which reflects the β-carboxylate of L-malate. Correcting for the latter gives a pK of 5.3 ± 0.4, similar to that observed with the wild-type enzyme (*4*). The maximum value in the pH−rate profile for V/K_{malate} is obtained at about pH 6, giving a pH-independent value of 4×10^3 M^{-1} s^{-1}, about 6% of that obtained for the wild-type enzyme, and K_{malate} is about 2-fold greater than that measured for the wild-type enzyme. As the pH is increased from 6, the rate constant decreases to a constant value of 355 M^{-1} s^{-1}, 10% the value at pH 6. The V/K_{malate} is then independent from pH 7.5 to pH 10. The estimated pK for the partial change is 6.3 ± 0.3, while the pK estimated for the parameter leveling off at a new constant value is 7.1 ± 0.3 (see analysis in Discussion).

The pH profiles for the Y126F mutant of malic enzyme are shown in Figure 2. The V/K pH−rate profile is qualitatively identical to the V/K pH profile for K199R. The maximum rate is seen at low pH and decreases to a constant value at high pH. The pK for the partial change is 6.7 ± 0.3. The rate at high pH is about 3-fold lower than the value at low pH, in contrast to K199R where the decrease is about 10-fold. The V profile also appears to show the same partial change in rate from low to high pH, and thus K_{malate} is nearly identical over this pH range. The average value of K_{malate} from pH 5.8 to pH .6 is 10 ± 2 mM and from pH 7.5 to pH 9.7 is 12 ± 2 mM. The pH-independent value of V at low pH is 0.0122 ± 0.0005 s^{-1} and decreases to 0.0046 ± 0.0007 s^{-1} at high pH, a 2.6-fold change. The pK for the partial change in the V profile is 6.6 ± 0.3. The V/K_{malate} profile decreases at low pH, giving a pK of 5.6 ± 0.3, but the V profile does not decrease at low pH.

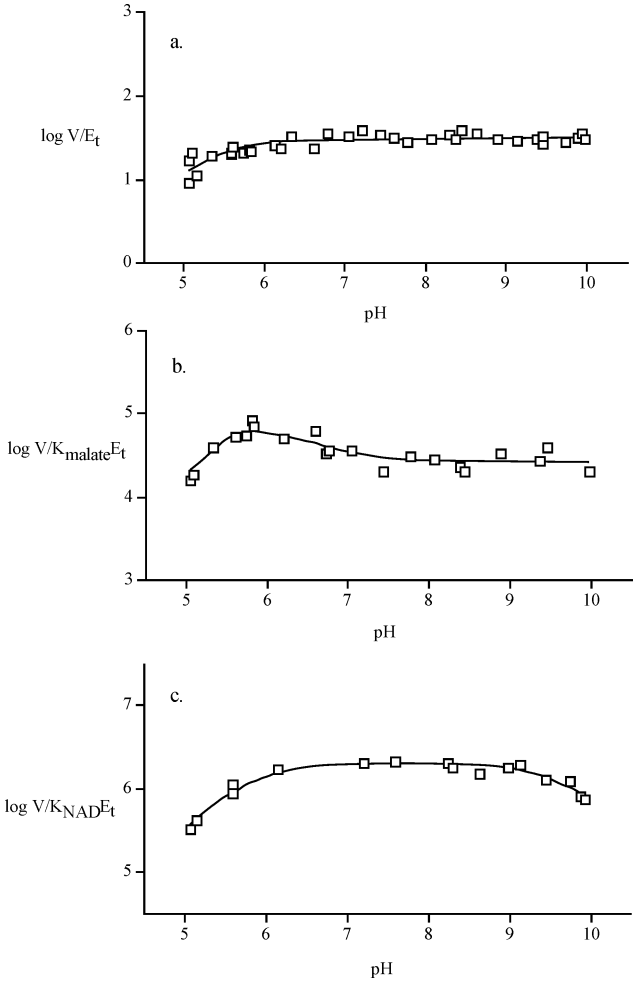

FIGURE 3: pH dependence of kinetic parameters for the recombinant wild-type enzyme. Initial rates were measured at saturating concentrations of NAD (0.5 mM) and Mg^{2+} (200 mM), and the malate concentration was varied from 0.5 to 5 mM for the V and the V/K_{malate} profiles. For the V/K_{NAD} profile, malate and Mg^{2+} were maintained at 50 and 200 mM, respectively, and the NAD concentration was varied from 0.01 to 0.1 mM. The concentration of the wild-type enzyme was 2.3 nM. Points are the experimental values, and the curves are based on a fit of the V (a) data to eq 5, V/K_{malate} (b) data to eqs 5 and 6, and V/K_{NAD} data to eq 4.

The similarity in the pH profiles for the K199R and Y126F mutant enzymes prompted a reinvestigation of the wild-type malic enzyme pH−rate profiles. An initial velocity pattern done at pH 9.7 varying Mg^{2+} and malate gave a dissociation constant for Mg^{2+} of about 11 mM, similar to the value of about 5 mM determined at pH 7 (*6*). Consequently, for the pH profile in the current work the free Mg^{2+} concentration was maintained at 200 mM throughout the pH profile. The V/K_{malate} pH profile for the wild-type enzyme is presented in Figure 3B and is qualitatively identical to the K199R and Y126F profiles. The maximum rate is seen at low pH and decreases by about 3-fold to a constant rate at high pH with a pK of 6.4 ± 0.8 for the partial change. No decrease in V/K_{malate} is observed up to a pH of 9.9. The activity decreases on the acid side below a pK of about 5.6. The V profile also decreases at low pH below a pK of 5.23 ± 0.06 and is presented in Figure 3A. The V/K_{NAD} pH−rate profile is shown in Figure 3C and shows two pK values of 5.72 ± 0.06 and 9.73 ± 0.08 at low and high pH, respectively.

The pH profiles obtained with the D294A mutant of malic enzyme are shown in Figure 4. The V/K_{malate} pH profile

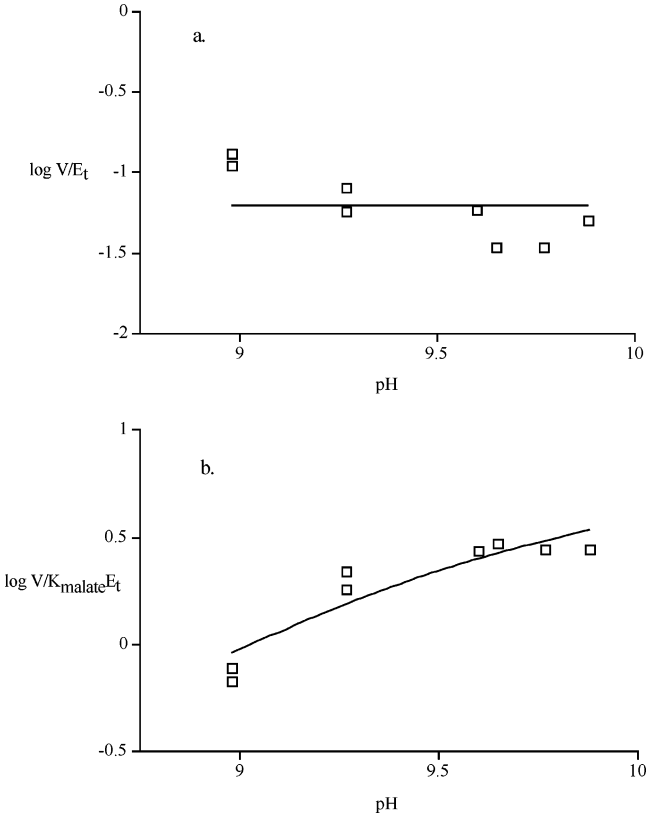

FIGURE 4: pH dependence of kinetic parameters for the D294A mutant enzyme. Initial rates were measured at saturating concentrations of NAD (0.5 mM) and Mg^{2+} (200 mM), and the malate concentration was varied from 2 to 50 mM. The D294A concentration was 0.8 μM. Points are the experimental values, and the curves are drawn by eye.

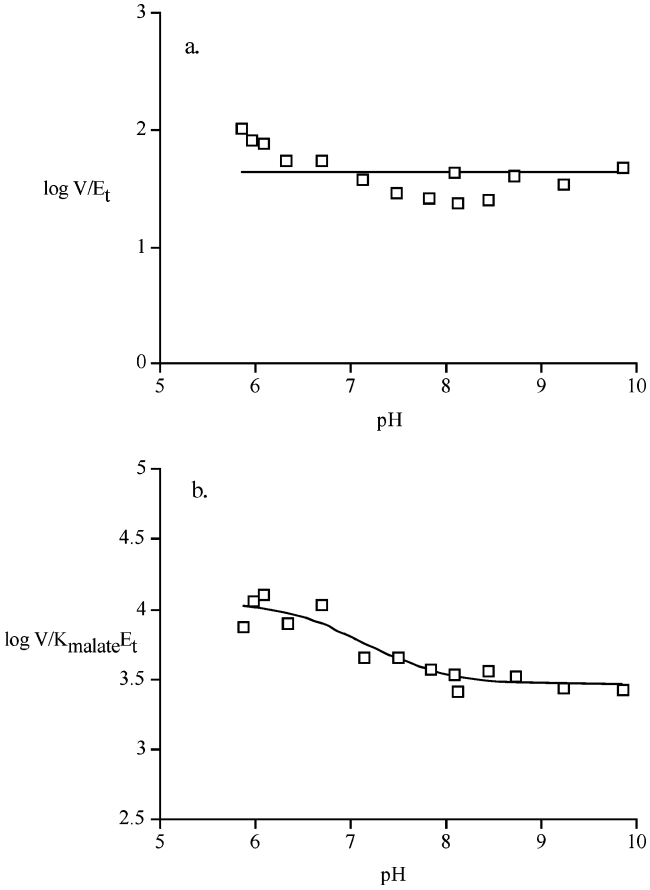

FIGURE 5: pH dependence of kinetic parameters for the R105A mutant enzyme. Initial rates were measured at saturating concentrations of NAD (0.5 mM) and Mg^{2+} (200 mM), and the malate concentration was varied from 3 to 40 mM. The concentration of R105A was 3 nM. Points are the experimental values, and the curves are based on a fit of the data for V/K_{malate} (b) data to eq 6.

indicates the D294A mutant is active only at high pH. The activity decreases as the pH decreases below a pK > 9, and the calculated pH-independent value of 5.5 ± 1.8 M^{-1} s^{-1} is about 13000-fold lower than that of the wild-type enzyme. A previous report suggested the D294A mutant of malic enzyme had only a 2000-fold decrease in V/K_{malate} compared to the wild-type enzyme at pH 7 (*6*). The apparently higher activity reported previously for D294A was likely due to contamination with *Escherichia coli* malic enzyme as a result of the manner in which the enzyme was previously purified. The V profile for the D294A mutant appears to be pH independent but does display some increase at lower pH. The pK and pH-independent values of the kinetic parameters from the $V/K_{malate}E_t$ pH−rate profiles for the wild-type and all the mutant enzymes are summarized in Table 1.

Fumarate and malate are allosteric activators of the *Ascaris* malic enzyme (*11*) that bind to separate activator sites (*22*). Arginine at position 105 forms two hydrogen bonds to one of the carboxylates of fumarate in the activator site (*23*). The R105A mutant enzyme does not show activation by either fumarate or malate (*22*). The R105A V/K_{malate} pH profile, Figure 5, displays the same partial activity loss as the wild-type enzyme. The decrease in activity from low pH to high pH is about 4-fold and has a pK of 6.8 ± 0.8 for the change. The V profile for R105A also appears to show about a 2-fold decrease in rate over the pH range investigated, but there is a significant error on the measured parameters. The malate saturation curves are linear above pH 5.5 but display significant positive cooperativity below pH 5.5, so data were not collected below this pH. The reason for the cooperativity at low pH is unknown at present.

Table 1: Summary of V/K_{malate} pH Data for Wild-Type and Mutant Malic Enzymes

enzyme	low pH pK[a]	partial activity loss pK[b]	Y_L	Y_H	R
wild type	5.6 ± 0.2	6.4 ± 0.8	(7.1 ± 0.6) × 10^4	(2.5 ± 0.2) × 10^4	2.8 ± 0.6
R105A		6.8 ± 0.8	(1.1 ± 0.1) × 10^4 (6.3)[c]	(2.8 ± 0.3) × 10^3 (8.9)	4.0 ± 0.6
K199R	5.3 ± 0.4	6.3 ± 0.3	4 × 10^3 (18)	355 (72)	11
Y126F	5.6 ± 0.2	6.7 ± 0.3	1.29 ± 0.05 (55000)	0.39 ± 0.02 (65000)	3.3 ± 0.3
D294A	>9		~6 (13000)		

[a] The pK values are from a fit of the data using eqs 5 and 6. [b] pK values are derived from a fit of the data using eq 6 for partial activity loss as a function of pH. Y_L and Y_H are the pH-independent values of V/KE_t expressed in M^{-1} s^{-1} at low and high pH, respectively, and R is the ratio of these values. [c] The number in parentheses is the fold change in the parameter compared to the wild-type enzyme.

Table 2: Isotope Effects for the K199R Mutant of Malic Enzyme

	$^{13}(V/K_{malate})_H$[a]	$^{13}(V/K_{malate})_D$[a]	^{D}V[b]	$^{D}(V/K_{malate})$[b]
WTME[c]	1.0342 ± 0.0002	1.0252 ± 0.0002	2.0 ± 0.2	1.6 ± 0.3
K199R (pH 6)	1.025 ± 0.001	1.017 ± 0.001	2.3 ± 0.2	2.2 ± 0.2
K199R (pH 9)	1.030 ± 0.001	1.023 ± 0.001	2.3 ± 0.4	2.1 ± 0.5

[a] Average of four determinations. [b] Average of three determinations. [c] Data are from refs *4* and *7*.

Isotope Effects. ^{D}V and $^{D}(V/K_{malate})$ values obtained for the K199R mutant enzyme are slightly larger than those obtained for the wild-type enzyme, whether measured at pH 6 or pH 9. Compared to the $^{13}(V/K_{malate})$ of the wild-type enzyme, the value of the K199R mutant enzyme at pH 6 is decreased from 3.4% to 2.5%, and deuteration of malate decreases it further to 1.7%. When the pH is increased from 6 to 9, $^{13}(V/K_{malate})$ for the K199R mutant enzyme increases to 1.03 and is decreased to 1.023 upon deuteration of malate. The primary deuterium isotope effects, ^{13}C isotope effects, and ^{13}C−deuterium multiple isotope effects are presented in Table 2.

DISCUSSION

pH−Rate Profiles for the Wild-Type Malic Enzyme. The malate pH−rate profile for V/KE_t decreases below a pH of 5.6, indicating an enzymatic group is required to be unprotonated for activity. A previously published pH profile for malic enzyme indicated two p*K* values on the acid side of the profile (*2*). One of these was attributed to a substrate p*K* and the second to an enzymatic group thought to be the general base in the reaction. The current work was not extended to low enough pH to reveal the substrate p*K*. The previous work indicated a p*K* value for the enzymatic group as 4.7, while the current study determined a p*K* value closer to 5.6. Although the absolute value of the p*K* is somewhat different, both studies indicate a requirement for a group to be unprotonated for activity that is likely the general base in the reaction. The current work also clearly shows a partial activity loss with a p*K* of about 6.5. A close inspection of the previously published *V*/*K* malate profile suggests the presence of this partial change in activity, but due to the relatively small change in activity it went undetected in the former work. The partial activity loss will be discussed more fully below in a separate section.

The major difference between the former work and the present is the absence of a p*K* on the basic side of the *V*/*K* pH profile presented in this study. A previously published V/K_{malate} pH profile for the wild-type enzyme suggested a bell-shaped profile with decreases at low and high pH and p*K* values of about 5 and 9, respectively (*2*). In the previous work the dissociation constant for Mg^{2+} was reported to decrease at high pH, and consequently, in doing the pH−rate profile, the metal ion concentration was decreased at high pH based upon the assumption of a decrease in the dissociation constant. Our current work suggests the Mg^{2+} dissociation constant does not change significantly with pH, and thus the previously reported decrease in V/K_{malate} at high pH was due to the lowering of the metal ion concentration rather than the ionization of an enzymatic group.

The proposed mechanism for malic enzyme requires a general acid to protonate the enolpyruvate intermediate to form pyruvate. The X-ray crystal structure of the human mitochondrial malic enzyme in complex with malate, Mn, and NADH suggests that tyrosine 126 in the *Ascaris* enzyme is likely the general acid. However, release of CO_2 occurs prior to the tautomerization step, and thus one would not expect to see the p*K* for the general acid in the *V*/*K* profile since the steps included in *V*/*K* end with the first irreversible step, which would be CO_2 release. One might expect to observe the p*K* in the *V* profile if the tautomerization step contributed to rate limitation. However, tautomerization is not slow. The *V* profile decreases on the acid side with a p*K* of about 5.2, similar to that observed in the *V*/*K* profile, and is pH independent from pH 6 to pH 10. The p*K* of 5.2 is similar to the p*K* of 4.8 reported in the previous work with NAD as the reactant. The p*K* on the acid side of the *V* profile has been attributed to a pH-dependent isomerization of E−NAD (*24*). The V/K_{NAD} profile displays two p*K* values at pH 5.7 and pH 9.7. The p*K* at 5.7 likely represents the general base in the reaction that is required to be unprotonated for activity. The V/K_{malate} profile represents ionizations for groups in the E−NAD−Mg complex and free malate, while the V/K_{NAD} profile represents ionizations of groups in the E−Mg−malate complex and free NAD. The p*K* on the basic side of the V/K_{NAD} profile likely represents a binding group for NAD since it is not observed in the *V* or V/K_{malate} profiles.

Y126F Mutant of Malic Enzyme. Three-dimensional structures of malic enzyme suggest Y126 is the general acid in the oxidative decarboxylation reaction and donates a proton to the enolpyruvate intermediate to form pyruvate. Consistent with a direct role for Y126 in catalysis, V/KE_t is decreased in Y126F about 60000-fold and V/E_t about 2600-fold compared to the wild-type enzyme. The Y126F mutation affects malate binding significantly as K_{malate} [K_m is equal to K_d for the wild-type enzyme (*2*, *5*) and should be in this case as well since the rate is several thousand fold lower] is increased at pH 6 about 20-fold compared to that of the wild-type enzyme. The shape of the Y126F *V*/*K* pH profile is essentially identical to that of the wild-type enzyme. The p*K* for the general base in the Y126F mutant enzyme is 5.6, the same as that observed for the wild-type enzyme, and implies Y126 does not play a role in lowering the p*K* for the general base in the reaction. Thus, none of the p*K*s observed for the wild-type enzyme reflect the Y126 hydroxyl, and the hydroxyl does not affect any of the active site p*K* values.

Converting tyrosine to phenylalanine will remove the general acid and would be expected to have the greatest effect on the rate of the tautomerization step. In the wild-type enzyme the tautomerization step is fast and not rate limiting but could contribute to rate limitation in the Y126F mutant. The significant decrease in activity of the Y126F mutant enzyme also may be related to the role of Y126 in closure of the active site upon binding malate. When substrates bind to the malic enzyme active site, domains B and C move closer to each other (*9*). These two domains, along with the long helix from domain A, bury the substrates deep in the

active site cavity and give the closed form of malic enzyme. When Y126 is replaced with F, the long helix loses one of the anchors that hold it between domains C and B. Therefore, the movement of domains B and C will result in an unusual position for the long helix of domain A. Thus Y126 is involved in closure of the active site, and upon closure of the active site Y126 moves to within hydrogen-bonding distance to K199, the putative general base in the reaction. The loss of this hydrogen bond in the Y126F mutant enzyme could indirectly affect the hydride transfer step by changing the position of K199 relative to the 2-hydroxyl of bound malate. A change in distance and/or orientation between K199 and substrate could affect the hydride transfer step and the proton shuttle role that K199 plays in catalysis. Consequently, the Y126F mutation could affect other steps in catalysis in addition to its primary role in the tautomerization step.

K199R Mutant of Malic Enzyme. The K199R mutant enzyme is the most active of the active site mutants investigated. The maximum velocity is decreased about 10-fold, and V/KE_t is decreased about 18-fold at pH 6 compared to the wild-type enzyme. At pH 6 the K_{malate} is about twice that of the wild-type enzyme even with the presence of the bulkier arginine in place of lysine. As for the wild-type enzyme the K_m increases at higher pH, but the change in K_m is about 10-fold in the case of K199R. Since V/K_{malate} is decreased less than 20-fold in K199R compared to the wild-type enzyme, it suggests the arginine is positioned reasonably well to act as the general base in place of lysine. As for the wild-type enzyme the general base must be unprotonated for activity, and the observed p*K* of pH 5.3 is within error equal to the p*K* for the general base in the wild-type enzyme. Since the p*K* is not shifted to higher pH with arginine replacing lysine, the p*K* of 5.3 is not that of K199. One possibility is that the group with a p*K* of 5.3 accepts a proton from K199 (or R199) to allow it to act as a base to accept a proton from the 2-hydroxyl of malate during hydride transfer. The most likely candidate for this group is D294. In the open form of malic enzyme K199 and D294 are within hydrogen-bonding distance, and K199 is likely protonated and D294 unprotonated given the large p*K* mismatch between the amino group of lysine and the carboxylate group of an aspartate. As the enzyme closes on binding substrates, additional hydrogen-bonding interactions are formed, and the general base must become unprotonated. On closure of the active site D294 moves to within about 2.8 Å of E271 and likely becomes protonated and hydrogen bonded to E271. The V/K_{malate} profile represents protonation/deprotonation events in the E−NAD−Mg complex. Under the initial velocity conditions employed in these studies the E−NAD−Mg complex is actually a complex with malate bound at the malate activator site, giving an activated enzyme (*24*). The E−NAD−Mg complex with malate at the activator site is in an open form with K199 hydrogen bonded solely to D294. Protonation of D294 would lead to loss of activity since K199 could not be deprotonated by D294, and the p*K* of about 5.6 is reasonable for an aspartate carboxylate group. In agreement with D294 being responsible for the p*K* of 5.6, the p*K* observed at low pH is not perturbed from pH 5.6 in the K199R or Y126F mutant enzymes.

D294A Mutant of Malic Enzyme. The D294A mutant enzyme is active only at high pH above 9.7, suggesting the general base p*K* is perturbed from about 5.6 in the wild-type enzyme to 9.7 in D294A. The V/E_t is reduced about 13000-fold compared to the wild-type enzyme, indicating the importance of D294 in catalysis. Although D294 is not in position to be directly involved in the acid−base mechanism of malic enzyme, it is within hydrogen-bonding distance to K199 in the closed form of the enzyme. The p*K* > 9 in D294A likely represents the largely unperturbed p*K* of K199 that is required to be unprotonated to accept the proton from the 2-hydroxyl of malate during hydride transfer. K_{malate} is increased about 10-fold in D294A. D294 does not interact directly with malate, so the increase in K_m is likely due to changes in the orientation of malate relative to active site residues that interact with malate to promote binding. The loss of the hydrogen-bonding interaction between D294 and K199 could affect the position and/or orientation of K199 relative to the 2-hydroxyl of malate and thus affect malate binding. The large loss in activity of D294A compared to the wild-type enzyme may be due to a change in the position of K199 relative to the 2-hydroxyl of malate so that hydride transfer occurs less efficiently. K199 also plays a role in other steps of the mechanism shuttling a proton between itself and the reaction intermediates. All of these steps could be affected by the mutation of D294.

Acid−Base Chemistry. The proposed overall mechanism of malic enzyme is shown in Scheme 2. Prior to binding malate, the enzyme is in an open conformation with a hydrogen-bonding interaction between K199 and D294 as these two residues are separated by about 2.5 Å (Scheme 2, I). Upon binding malate and closure of the active site an additional hydrogen-bonding interaction is formed between K199 and Y126, and a proton is transferred to D294 as it comes in close proximity to E271 (Scheme 2, II). Although E271 is a ligand for the Mg^{2+}, it will still have a partial negative charge. There are four negatively charged carboxylates coordinated to the metal ion, D295, D272, E271, and the α-carboxylate of malate, and these are only partially neutralized by the metal ion and R181, which is within hydrogen-bonding distance to the α-carboxylate of malate. Thus, K199, within hydrogen-bonding distance to the α-hydroxyl of malate, accepts a proton from the 2-hydroxyl of malate in the hydride transfer step (Scheme 2, II). Hydride transfer leads to the oxalacetate intermediate, which is then decarboxylated with a Lewis acid assist from the bound metal ion. During the decarboxylation step a proton is shuttled from K199 to the carbonyl oxygen of oxalacetate to form enolpyruvate (Scheme 2, III). The tautomerization step basically involves general base−general acid catalysis and may occur in two steps (Scheme 2, IV). The end result is that K199 accepts a proton from the enol hydroxyl, and this coincides with protonation of C3 of pyruvate by Y126 (Scheme 2, V). Release of pyruvate and NADH then regenerates enzyme in the correct protonation state for another catalytic cycle (Scheme 2, VI).

The 10-fold change in V, observed when R replaces K, results from the increased p*K* for R. The full effect of about 100-fold (the solution p*K* for K is 2 pH units lower than R) is not seen since the chemical steps are not completely rate limiting for the wild-type enzyme (*5*).

Partial Activity Change. What is the identity of the group with a p*K* of about 6.5 that affects malate binding in the wild-type and K199R mutant enzyme? The pH dependence

Scheme 2: Proposed Acid−Base Mechanism of *A. suum* NAD−Malic Enzyme

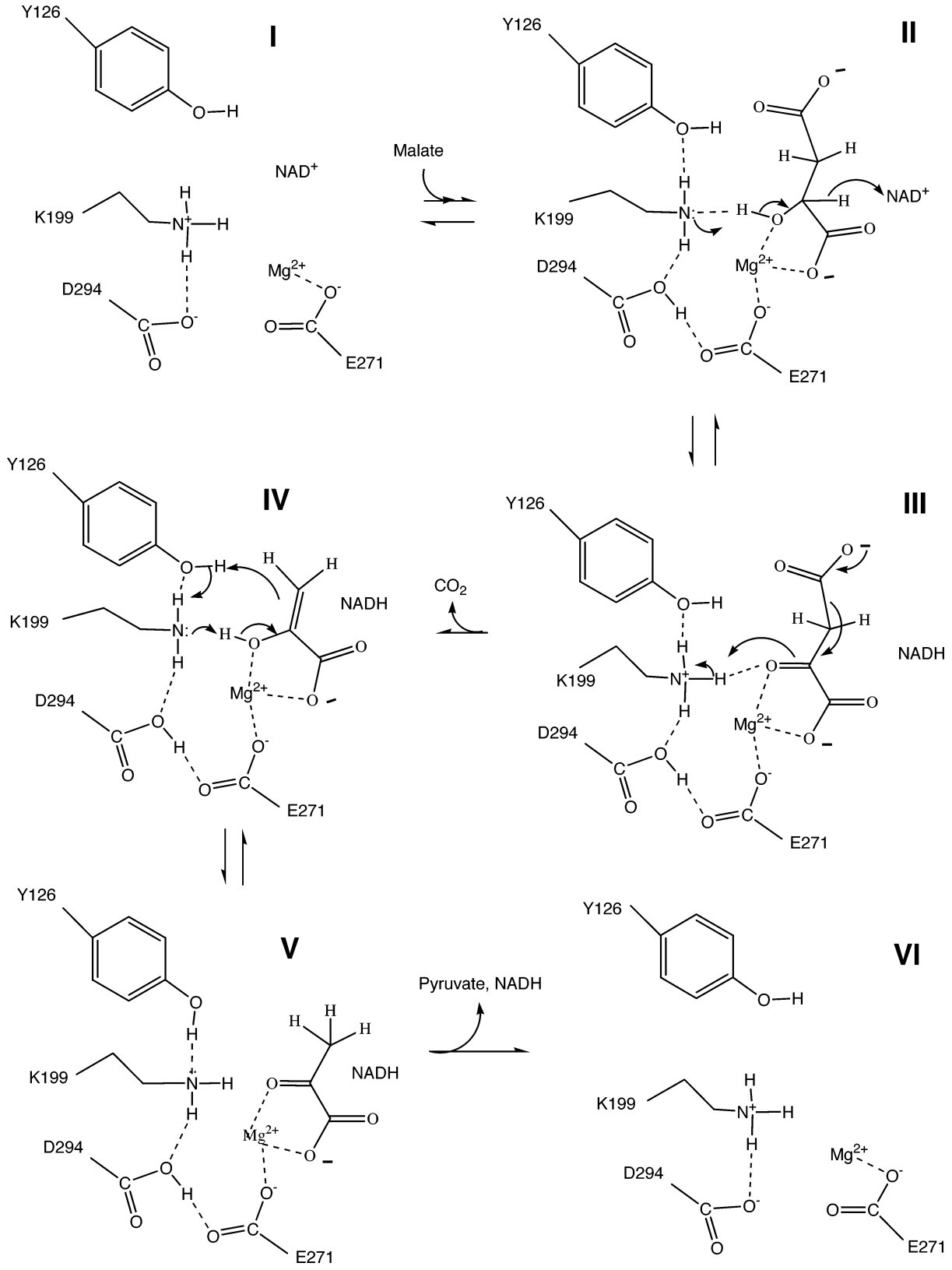

is observed for the wild-type enzyme, and thus the residue is important for the binding of malate in the wild-type enzyme and the K199R mutant. The K_m for malate is its K_d in the case of the wild-type enzyme (*2*), and this must also be true for the K199R mutant enzyme since V/E_t has decreased 10-fold compared to that of the wild-type enzyme. From the data in Figure 1, a value of about 1 mM is estimated graphically for $K_{i\ malate}$ (the ratio of V and V/K_{malate}) and pK_3 is approximately 6.3, while $K_{j\ malate}$ is about 10 mM. Thus, the affinity of enzyme for malate is decreased 10-fold when the group with a pK of 6.3 is unprotonated in the K199R mutant enzyme, and the group's pK is perturbed from about 6 to about 7 when malate is bound to enzyme. For the wild-type enzyme the affinity of enzyme for malate is decreased about

3-fold when the group is unprotonated, and the pK values are very similar.

In contrast, the partial activity change observed for the Y126F mutant enzyme is on V rather than on V/K. The effects on V for Y126F could be on catalytic steps or on product release steps, but since K_{malate} is increased more than 20-fold by the mutation, it is unlikely that release of pyruvate would become more limiting. Also, since there is such a large decrease in rate for the Y126F enzyme compared to the wild type, it suggests that the catalytic steps are limiting for this mutant enzyme. The tautomerization step may be the slowest step along the reaction pathway for Y126F and, thus, may be the step affected by the partial activity change (this aspect is now being pursued).

The partial activity change is not observed in the V/K_{NAD} profile, and thus it seems to rule out the possibility that the ionization state of a group in the NAD binding site has an effect on malate binding. The *Ascaris* malic enzyme is activated by malate and fumarate, and each binds to separate allosteric activator sites. The activation by either of the activators results from an increase in the affinity of the enzyme for malate and metal ion in the presence of the activator (*22*). The possibility that the group whose ionization state affects malate binding could be related to the malate or fumarate activation properties was investigated by studying the pH dependence of the R105A mutant. Arginine 105 is in the fumarate activator site and donates two hydrogen bonds to fumarate. The R105A mutant enzyme is not activated by either fumarate or malate and displays the same partial activity change as the wild-type enzyme. Data suggest the partial change is not directly related to the allosteric activator properties of malic enzyme.

Other than the ligands to the metal ion and the members of the catalytic triad, there are only a few residues that interact with malate, N433, N478, and R181, and none of these are ionizable around pH 6. Therefore, it does not appear that any of the groups that line the active site are likely involved in the partial activity change. The group whose ionization state affects activity is probably remote from the active site and is transmitted through the protein to the active site by a conformational change.

$$\text{E·MA} \underset{k_6}{\overset{k_5\text{B}}{\rightleftharpoons}} \text{E·MAB} \underset{k_8}{\overset{k_7}{\rightleftharpoons}} \text{(E·MAB)} \underset{k_{10}}{\overset{k_9}{\rightleftharpoons}} \text{E·MXR} \overset{k_{11}}{\rightleftharpoons} \quad (9)$$

Isotope Effects. For both the wild-type malic enzyme and the K199R mutant enzyme, mechanism 9 holds (*7*), where M is Mg^{2+}, A is NAD, B is malate, and X is oxalacetate. In the above scheme, k_5 and k_6 represent binding and dissociation of malate, k_7 and k_8 reflect a conformational change (isomerization), k_9 and k_{10} represents hydride transfer, and k_{11} represents decarboxylation. At saturating substrate concentration, oxidative decarboxylation and isomerization of the E·NAD complex contribute to rate limitation (*5*, *24*). As a result, we do not include steps for release of pyruvate or NADH. Based on mechanism 9, equations for the isotope effects can be written as follows:

$$^{D}V = \frac{^{D}k_9 + C_{Vf} + C_r(^{D}K_{eq})}{1 + C_{Vf} + C_r} \quad (10)$$

$$^{D}\left(\frac{V}{K_{malate}}\right) = \frac{^{D}k_9 + C_f + C_r(^{D}K_{eq})}{1 + C_f + C_r} \quad (11)$$

$$^{13}\left(\frac{V}{K_{malate}}\right)_H = \frac{^{13}k_{11} + (1 + C_f)/C_r}{1 + (1 + C_f)/C_r} \quad (12)$$

$$^{13}\left(\frac{V}{K_{malate}}\right)_D = \frac{^{13}k_{11} + (^{D}k_9 + C_f)/C_r(^{D}K_{eq})}{1 + (^{D}k_9 + C_f)/C_r(^{D}K_{eq})} \quad (13)$$

where $^{D}k_9$ and $^{13}k_{11}$ represent intrinsic primary deuterium and ^{13}C isotope effects, $^{D}K_{eq}$ is the equilibrium isotope effect [1.18 in the case of malic enzyme (*21*)], $C_f = (k_9/k_8)(1 + k_7/k_6)$, $C_{Vf} = (k_9/k_7 + k_9/k_{11})/(1 + k_8/k_7)$, and $C_r = k_{10}/k_{11}$.

All observed isotope effects reflect changes in the catalytic conformational change that precedes oxidative decarboxylation, hydride transfer, and decarboxylation. The wild-type malic enzyme reaction has a stepwise mechanism in which the hydride transfer step precedes the decarboxylation step. The stepwise mechanism requires $^{13}(V/K_{malate})_H > {}^{13}(V/K_{malate})_D$, and this inequality is satisfied at both pH 6 and pH 9, so the stepwise mechanism does not change upon making the K199R mutant enzyme, nor is the stepwise mechanism affected by the partial activity change. The primary deuterium isotope effect is increased to about 2.2 in the K199R mutant compared to 1.6 in the wild-type enzyme. The increase in the deuterium isotope effect for K199R suggests that the hydride transfer step has become more rate limiting in the mutant enzyme and is consistent with the proposed role of K199 as the general base in the reaction. The $^{13}(V/K)$ isotope effect at pH 6 is decreased compared to the wild-type enzyme, and the simplest explanation is that the decrease results from a greater rate limitation by hydride transfer. The $^{13}(V/K)$ isotope effect for K199R increases from 2.5% at pH 6 to 3% at pH 9. This cannot be due to a change in the commitment factors alone, because this would also show a change in $^{D}(V/K)$. The reason for the change in $^{13}(V/K)$ is now being pursued.

REFERENCES

1. Karsten, W. E., and Cook, P. F. (2000) Pyridine Nucleotide-Dependent β-Hydroxyacid Oxidative Decarboxylases: An Overview, *Protein Pept. Lett. 7*, 281−286.
2. Kiick, D. M., Harris, B. G., and Cook, P. F. (1986) Protonation Mechanism and Location of Rate-Determining Steps for the *Ascaris suum* Nicotinamide Adenine Dinucleotide-Malic Enzyme Reaction from Isotope Effects and pH Studies, *Biochemistry 25*, 227−236.
3. Park, S.-H., Harris, B. G., and Cook, P. F. (1986) pH Dependence of Kinetic Parameters for Oxalacetate Decarboxylation and Pyruvate Reduction Reactions Catalyzed by Malic Enzyme, *Biochemistry 25*, 3752−3759.
4. Weiss, P. M., Gava, S. R., Harris, B. G., Urbauer, J. L., Cleland, W. W., and Cook, P. F. (1991) Multiple Isotope Effects with Alternative Dinucleotide Substrates as a Probe of the Malic Enzyme Reaction, *Biochemistry 30*, 5755−5763.
5. Karsten, W. E., and Cook, P. F. (1994) Stepwise versus Concerted Oxidative Decarboxylation Catalyzed by Malic Enzyme: A Reinvestigation, *Biochemistry 33*, 2096−2103.
6. Karsten, W. E., Chooback, L., Liu, D., Hwang, C.-C., Lynch, C., and Cook, P. F. (1999) Mapping the Active Site Topography of the NAD-Malic Enzyme via Alanine-Scanning Site-Directed Mutagenesis, *Biochemistry 38*, 10527−10532.
7. Liu, D., Karsten, W. E., and Cook, P. F. (2000) Lysine 199 Is the General Acid in the NAD-Malic Enzyme Reaction, *Biochemistry 39*, 11955−11960.

8. Coleman, D. E., Rao, G. S. J., Goldsmith, E. J., Cook, P. F., and Harris, B. G. (2002) Crystal Structure of the Malic Enzyme from *Ascaris suum* Complexed with Nicotinamide Adenine Dinucleotide at 2.3 Å Resolution, *Biochemistry 41*, 6928−6938.
9. Yang, Z., Floyd, D., Loeber, G., and Tong, L. (2000) Structure of a Closed Form of Human Malic Enzyme and Implications for Catalytic Mechanism, *Nat. Struct. Biol. 7*, 251−257.
10. Xu, Y., Bhargava, G., Wu, H., Loeber, G., and Tong, L. (1999) Crystal Structure of Human Mitochondrial $NAD(P)^+$-dependent Malic Enzyme: A New Class of Oxidative Decarboxylases, *Structure 7*, 877−889.
11. Mallick, S., Harris, B. G., and Cook, P. F. (1991) Kinetic Mechanism of NAD:Malic Enzyme from *Ascaris suum* in the Direction of Reductive Carboxylation, *J. Biol. Chem. 266*, 2732−2738.
12. Yang, Z., and Tong, L. (2000) Structural Studies of a Human Malic Enzyme, *Protein Pept. Lett. 7*, 287−296.
13. Tao, X., Yang, Z., and Tong, L. (2003) Crystal Structures of Substrate Complexes of Malic Enzyme and Insights into the Catalytic Mechanism, *Structure 11*, 1141−1150.
14. Chang, G.-G., and Tong, L. (2003) Structure and Function of Malic Enzymes, A New Class of Oxidative Decarboxylases, *Biochemistry 42*, 12721−12733.
15. Bradford, M. M. (1976) A Rapid and Sensitive Method for the Quantitation of Microgram Quantities of Protein Utilizing the Principle of Protein-Dye Binding, *Anal. Biochem. 72*, 248−254.
16. Viola, R. E., Cook P. F., and Cleland, W. W. (1979) Stereoselective Preparation of Deuterated Reduced Nicotinamide Adenine Nucleotides and Substrates by Enzymatic Synthesis, *Anal. Biochem. 96*, 334−340.
17. Park, S.-H., Kiick, D. M., Harris, B. G., and Cook, P. F. (1984) Kinetic mechanism in the direction of oxidative decarboxylation for NAD-malic enzyme from *Ascaris suum*, *Biochemistry 23*, 5446−5453.
18. O'Leary, M. H. (1980) Determination of Heavy-Atom Isotope Effects on Enzyme-Catalyzed Reactions, *Methods Enzymol. 64*, 83.
19. Cleland, W. W. (1979) Statistical Analysis of Enzyme Kinetic Data, *Methods. Enzymol. 63*, 103−138.
20. Northrop, D. B. (1975) Steady-State Analysis of Kinetic Isotope Effects in Enzyme Reactions, *Biochemistry 14*, 2644−2651.
21. Cook, P. F., and Cleland, W. W. (1981) Mechanistic Deductions from Isotope Effects in Multireactant Enzyme Mechanisms, *Biochemistry 20*, 1790−1796.
22. Karsten, W. E., Pais, J. E., Rao, J., Harris, B. G., and Cook, P. F. (2003) *Ascaris suum* NAD-Malic Enzyme Is Activated by L-Malate and Fumarate Binding to Separate Allosteric Sites, *Biochemistry 42*, 9712−9721.
23. Yang, Z., Lanks, C. W., and Tong, L. (2002) Molecular Mechanism for the Regulation of Human Mitochondrial $NAD(P)^+$-Dependent Malic Enzyme by ATP and Fumarate, *Structure 10*, 951−960.
24. Rajapaksa, R., Abu-Soud, H., Raushel, F. M., Harris, B. G., and Cook, P. F. (1993) Pre-Steady-State Kinetics Reveal a Slow Isomerization of the Enzyme-NAD Complex in the NAD-Malic Enzyme Reaction, *Biochemistry 32*, 1928−1934.

BI047826O